Inorg. Chem. **2009**, *48*, 4219−4230

Cadmium(II) Cysteine Complexes in the Solid State: A Multispectroscopic Study

Farideh Jalilehvand,*,† Vicky Mah,† Bonnie O. Leung,† János Mink,‡,§ Guy M. Bernard,|| and László Hajba§

Department of Chemistry, University of Calgary, Calgary, AB, Canada T2N 1N4, Department of Molecular Spectroscopy, Chemical Research Center of the Hungarian Academy of Sciences, P.O. Box 17, H-1525 Budapest, Hungary, Research Institute of Chemical and Process Engineering, Faculty of Information Technology, University of Pannonia, P.O. Box 158, H-8201 Veszprém, Hungary, and Department of Chemistry, University of Alberta, Edmonton, AB, Canada T6G 2G2

Received January 22, 2009

Cadmium(II) cysteinate compounds have recently been recognized to provide an environmentally friendly route for the production of CdS nanoparticles, used in semiconductors. In this article, we have studied the coordination for two cadmium(II) cysteinates, $Cd(HCys)_2 \cdot H_2O$ (**1**) and $\{Cd(HCys)_2 \cdot H_2O\}_2 \cdot H_3O^+ClO_4^-$ (**2**), by means of vibrational (Raman and IR absorption), solid-state NMR (^{113}Cd and ^{13}C), and Cd K- and L_3-edge X-ray absorption spectroscopy. Indistinguishable Cd K-edge extended X-ray absorption fine structure (EXAFS) and Cd L_3-edge X-ray absorption near edge structure (XANES) spectra were obtained for the two compounds, showing similar local structure around the cadmium(II) ions. The vibrational spectra show that the cysteine amine group is protonated (NH_3^+) and not involved in bonding. The ^{113}Cd solid-state cross-polarization magic angle spinning NMR spectra showed a broad signal in the ∼500−700 ppm range, with the peak maximum at about 650 ppm, indicating three to four coordinated thiolate groups. Careful analyses of low-frequency Raman and far-IR spectra revealed bridging and terminal Cd−S vibrational bands. The average Cd−S distance of 2.52 ± 0.02 Å that constantly emerged from least-squares curve-fitting of the EXAFS spectra is consistent with CdS_4 and CdS_3O coordination. Both structural models yielded reasonable values for the refined parameters, with a slightly better fit for the CdS_3O configuration, for which the Cd−O distance of 2.27 ± 0.04 Å was obtained. The Cd L_3-edge XANES spectra of **1** and **2** resembled that of the CdS_3O model compound and showed that the coordination around Cd(II) ions in **1** and **2** cannot be exclusively CdS_4. The small separation of 176 cm^{-1} between the infrared symmetric and antisymmetric COO^- stretching modes indicates monodentate or strongly asymmetrical bidentate coordination of a cysteine carboxylate group in the CdS_3O units. The combined results are consistent with a "cyclic/cage" type of structure for both the amorphous solids **1** and **2**, composed of CdS_4 and CdS_3O units with single thiolate (Cd−S−Cd) bridges, although a minor amount of cadmium(II) sites with CdS_3O_{2-3} and CdS_4O coordination geometries cannot be ruled out.

Introduction

Sulfide and selenide semiconductors attract considerable interest due to their optical and electronic properties.[1] A low cost and environmentally friendly route to prepare metal sulfide semiconductors could be via nanoparticles, synthesized by using small biomolecules such as cysteine as a source of sulfur.[2−4] CdS nanoparticles, widely used in optical devices, can be prepared using cysteine and salts of cad-

* To whom correspondence should be addressed. Email: faridehj@ucalgary.ca.
† University of Calgary.
‡ Chemical Research Center of the Hungarian Academy of Sciences.
§ University of Pannonia.
|| University of Alberta.

(1) Wang, X.; Zhuang, J.; Peng, Q.; Li, Y. *Langmuir* **2006**, *22*, 7364–7368.
(2) Zhang, B.; Ye, X.; Dai, W.; Hou, W.; Xie, Y. *Chem.—Eur. J.* **2006**, *12*, 2337–2342.
(3) Zhang, B.; Ye, X.; Hou, W.; Zhao, Y.; Xie, Y. *J. Phys. Chem. B.* **2006**, *110*, 8978–8985.
(4) Chen, X.; Zhang, X.; Shi, C.; Li, X.; Qian, Y. *Solid State Commun.* **2005**, *134*, 613–615.

10.1021/ic900145n CCC: $40.75
Published on Web 04/07/2009

Scheme 1. Previously Proposed Structures for $Cd(HCys)_2$ (left) and $[Cd\{Cd(HCys)_2\}_2][CdCl_4]$ (right)[7,9]

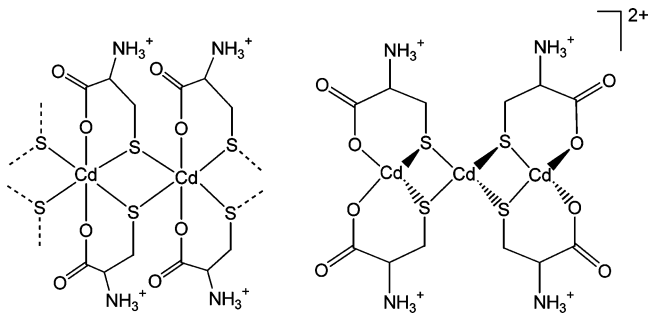

mium(II) nitrate or chloride as precursors.[5,6] Through a solvothermal process, Zhao and Huang obtained netted spherelike CdS nanostructures with sizes depending on the temperature (120−220 °C) as well as the Cd(II)/cysteine ratio and concluded that the CdS nanoparticles resulted from decomposition of the cadmium(II)−cysteine complexes at elevated temperatures.[6]

The structure of the cadmium(II) cysteine complexes is still an open question. Shindo and Brown obtained a 1:1 precipitate at pH ∼ 2 from equimolar amounts of $CdCl_2$ and cysteine, with the empirical composition Cd(HCys)Cl. On the basis of vibrational IR spectroscopic data, they proposed mixed CdS_4 and CdS_2O_2 coordination in a $[Cd\{Cd(HCys)_2\}_2][CdCl_4]$ structure (Scheme 1, right).[7] The crystal structure of $[Cd(HPen)Br(H_2O)]\cdot 2H_2O$ (H_2Pen = penicillamine or 3,3′-dimethylcysteine) showed six-coordinated cadmium(II) ions surrounded by two bridging bromine atoms, a thiolate group from one penicillamine ligand, two oxygen atoms of the COO^- group of another penicillamine molecule, and a water oxygen atom.[8] Barrie et al. performed a solid-state ^{113}Cd NMR study on a dehydrated $Cd(HCys)_2$ compound, prepared by mixing cadmium(II) acetate and cysteine in the molar ratio 1:2, and proposed a polymeric structure with six-coordinated cadmium(II) ions, see Scheme 1 (left).[9]

In this work, we have developed a structural model for two solid cadmium(II)−cysteine compounds, $Cd(HCys)_2\cdot H_2O$ (**1**) and $\{Cd(HCys)_2\cdot H_2O\}_2\cdot H_3O^+ClO_4^-$ (**2**), prepared from cadmium(II) acetate and perchlorate salts, respectively, based on results from a combination of spectroscopic methods.

Experimental Section

Sample Preparation. Cadmium(II) perchlorate hydrate, $Cd(ClO_4)_2\cdot 6H_2O$, cadmium(II) acetate hydrate, $Cd(CH_3COO)_2\cdot 2H_2O$, and L-cysteine (H_2Cys, $HO_2CCH(NH_2)CH_2SH$), were purchased from Sigma Aldrich and used without further purification. In order to prevent the oxidation of cysteine to cystine, samples were prepared under an argon atmosphere using water that had been boiled and purged with Ar to remove dissolved oxygen. The pH was monitored with a Corning Semi-Micro electrode.

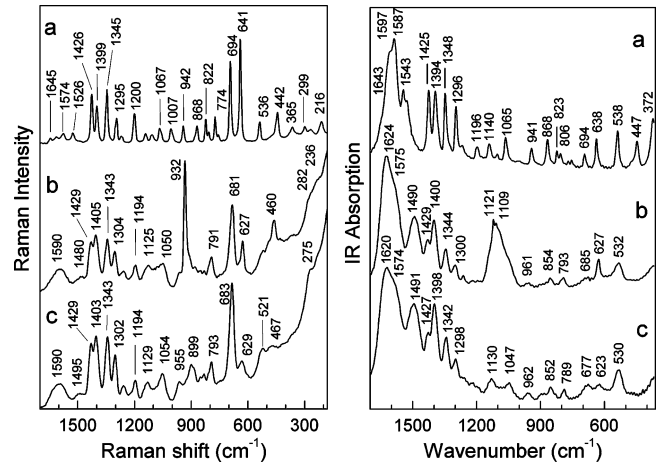

Figure 1. Raman (left) and IR (right) spectra of solid (a) cysteine zwitterions, (b) $\{Cd(HCys)_2\cdot H_2O\}_2\cdot H_3O^+ClO_4^-$ (**2**), and (c) $Cd(HCys)_2\cdot H_2O$ (**1**).

Cadmium(II) Cysteinate Solids. Cadmium(II) cysteinate, $Cd(HCys)_2\cdot H_2O$, was prepared as previously described:[9] 0.54 g (2.0 mmol) of cadmium(II) acetate hydrate was added to a solution of cysteine (0.48 g, 4.0 mmol) in 7 mL of oxygen-free water. A white precipitate immediately formed (pH = 2.7), which was filtered, washed with water and ether, and dried in a vacuum. Anal. calcd for $Cd(HCys)_2\cdot 1.05H_2O$ ($CdC_6H_{14.1}N_2O_{5.05}S_2$): C, 19.40; H, 3.83; N, 7.54. Found: C, 19.24; H, 3.53; N, 7.00. DSC/TGA: 52−143 °C, 5.14% obsd for loss of water.

A similar synthesis was performed using cadmium(II) perchlorate hydrate, and the precipitate formed (pH = 1.6) was filtered, washed with water and ether, and dried in a vacuum. Anal. calcd for $\{Cd(HCys)_2\cdot H_2O\}_2\cdot H_3O^+ClO_4^-$ ($Cd_2C_{12}H_{31}N_4O_{15}S_4Cl$): C, 16.76; H, 3.16; N, 6.51. Found: C, 16.47; H, 3.22; N, 6.18. DSC/TGA: 52−187 °C, 4.86% obsd for loss of water. Raman and IR spectra of the solid confirmed the presence of perchlorate ions in the compound (Figure 1; Tables S-1 and S-2 and Figure S-1, Supporting Information). Attempts to crystallize these highly insoluble solids failed.

Cadmium Reference Compounds. The crystalline compounds cadmium(II) perchlorate hydrate $Cd(ClO_4)_2\cdot 6H_2O$ (as CdO_6 coordination model), hexakis(*N*,*N*-dimethylthioformamide) cadmium(II) perchlorate $[Cd(SCHN(CH_3)_2)_6](ClO_4)_2$ (CdS_6 model),[10] tetraphenylphosphonium-tris(thioacetato) cadmate(II) $[Ph_4P][Cd(SCO(CH_3))_3]$ (CdS_3O_3 model),[11] cadmium adamantane cage $(Et_3NH)_4[S_4Cd_{10}(SPh)_{16}]$ (CdS_4 model),[12] bis(thiosaccharinato)-bis(imidazole) cadmium(II) $[Cd(tsac)_2(Im)_2]$ (CdS_2N_2 model),[13] imidazolium tris(thiosaccharinato)aqua cadmate(II) $(HIm)[Cd(tsac)_3(H_2O)]$ (CdS_3O model),[13] bis(nitrato)-bis(tetramethylthiourea) cadmium(II) $[Cd(tmtu)_2(NO_3)_2]$ (CdS_2O_4 model I),[14] bis(nitrato)-bis(thiourea) cadmium(II) $[Cd(tu)_2(NO_3)_2]$ (CdS_2O_4 model II),[15] bis(cysteaminate) cadmium(II) $[Cd(SCH_2CH_2NH_2)_2]$ (CdS_3N_2 model),[16] and bis(thiourea) cadmium(II) formate $[Cd(tu)_2(HCOO)_2]$ (CdS_4O_2 model)[17] were synthesized as previously described and verified by obtaining

(5) Barglik-Chory, C.; Remenyi, C.; Strohm, H.; Müller, G. *J. Phys. Chem. B.* **2004**, *108*, 7637–7640.
(6) Zhao, P.; Huang, K. *Cryst. Growth Des.* **2008**, *8*, 717–722.
(7) Shindo, H.; Brown, T. L. *J. Am. Chem. Soc.* **1965**, *87*, 1904–1909.
(8) Carty, A. J.; Taylor, N. J. *Inorg. Chem.* **1977**, *16*, 177–181.
(9) Barrie, P. J.; Gyani, A.; Motevalli, M.; O'Brien, P. *Inorg. Chem.* **1993**, *32*, 3862–3867.
(10) Stålhandske, C. M. V.; Stålhandske, C. I.; Sandström, M.; Persson, I. *Inorg. Chem.* **1997**, *36*, 3167–3173.
(11) Sampanthar, J. T.; Deivaraj, T. C.; Vittal, J. J.; Dean, P. A. W. *J. Chem. Soc., Dalton Trans.* **1999**, 4419–4423.
(12) Lee, G. S. H.; Fisher, K. J.; Vassallo, A. M.; Hanna, J. V.; Dance, I. G. *Inorg. Chem.* **1993**, *32*, 66–72.
(13) Tarulli, S. H.; Quinzani, O. V.; Baran, E. J.; Piro, O. E.; Castellano, E. E. *J. Mol. Struct.* **2003**, *656*, 161–168.
(14) Honkonen, R. S.; Marchetti, P. S.; Ellis, P. D. *J. Am. Chem. Soc.* **1986**, *108*, 912–915.

the unit cell dimensions from X-ray crystallography for their known structures, Figure S-7 (Supporting Information).

Vibrational Spectroscopy. The Raman spectra (range 100−3500 cm^{-1}, resolution 4 cm^{-1}, 1000 co-added scans) were recorded by means of a Bruker FRA 106 FT-Raman system equipped with a liquid-nitrogen-cooled Ge detector, exposing the solids contained in closed vials to the 1064 nm line (500 mW) from a YAG laser. The IR spectra (range 360−4000 cm^{-1}, 4 cm^{-1} resolution, 1000 co-added scans) were measured using a Bruker Vertex70 FT-IR spectrometer equipped with a KBr beamsplitter and deuterotriglycine sulfate (DTGS) detector. Far-infrared spectra (50−700 cm^{-1}) were recorded from polyethylene pellets with a Bio-Rad (Digilab) FTS-40 spectrometer equipped with an air-bearing interferometer, wire-mesh beamsplitter, high-pressure mercury source, and DTGS detector.

Solid-State ^{113}Cd and ^{13}C NMR Spectroscopy. Solid-state cross-polarization magic angle spinning (CP MAS) experiments were carried out on a Bruker AMX300 spectrometer equipped with a BL4 MAS double-resonance broadband probe at resonance frequencies of 75.48 MHz for ^{13}C and 66.59 MHz for ^{113}Cd nuclei. The samples were packed into 4 mm ZrO rotors with MAS rates between 4 and 6 kHz (2 and 5 kHz for the $[Cd(tu)_2(HCOO)_2]$ compound; tu = thiourea). The Hartmann−Hahn condition for ^{13}C experiments was optimized using solid glycine, which was also employed for secondary calibration by setting its carboxylate resonance to 176.2 ppm with respect to TMS.[18] Spectra were acquired using a 4 μs ^{1}H 90° pulse, 1 ms contact time, and 4 s recycle delay. For ^{113}Cd experiments, solid $Cd(ClO_4)_2 \cdot 6H_2O$ was used for calibration to 0 ppm and to set the Hartmann−Hahn condition.[19] Spectra were acquired using a 4 μs ^{1}H 90° pulse, 4 ms contact time, and 7 s recycle delay. For the $[Cd(tu)_2(NO_3)_2]$ and $[Cd(tu)_2(HCOO)_2]$ solids, the principal components of the shielding tensors ($\delta_{11} \geq \delta_{22} \geq \delta_{33}$) were obtained by the method of Herzfeld and Berger,[20] using the HBA 1.5 program.[21] The output parameters were then used to simulate the spectra by means of the WSOLIDS 1 program.[22]

X-Ray Absorption Spectroscopy. Cadmium K-edge extended X-ray absorption fine structure (EXAFS) data were collected at beamline 2-3 at the Stanford Synchrotron Radiation Lightsource (SSRL) under dedicated conditions of 3.0 GeV and 70−100 mA. Higher harmonics were rejected by detuning the Si[220] double-crystal monochromator to discard 50% of the maximum incident beam intensity. The spectra were recorded in transmission mode, with argon in the first ion chamber (I_0), and krypton in the second (I_1) and third (I_2) ion chambers. Solid samples were ground finely, combined with BN, and placed in a 1 mm aluminum frame sealed with Mylar tape. Three to five scans were collected for each sample and averaged after external calibration of their energy scale by assigning the first inflection point of the Cd K-edge of a Cd foil to 26711.0 eV.

The Cd L_3-edge X-ray absorption near edge structure (XANES) measurements were performed at beamline 9-A of the High Energy Accelerator Research Organization (Photon Factory), Tsukuba, Japan. The ring operates under dedicated conditions at 2.5 GeV and 350−400 mA. The data were collected in fluorescence mode with helium in the first ion chamber (I_0) and an argon-filled Lytle detector (I_f). Higher harmonics through the Si[111] double crystal monochromator were rejected by means of nickel- and rhodium-coated mirrors. The cadmium(II) cysteine samples and crystalline reference compounds were ground finely and dusted onto Mylar tape. For each sample, two to three scans were collected and averaged after external energy calibration relative to the first inflection point of the Cd L_3-edge of a Cd foil at 3537.6 eV.

XAS Data Analysis. The data treatment was performed using WinXAS 3.1.[23] The background absorption was subtracted with a first-order polynomial over the pre-edge region, followed by normalization of the edge step. For the Cd K-edge XAS spectra, the energy scale was converted into k space, where $k = (8\pi^2 m_e/h^2)(E - E_0)$, using a threshold energy of $E_0 = 26710.8$ eV for both solids. The EXAFS oscillation was then extracted using a seven-segment cubic spline.

The EXAFS model functions, $\chi(k)$, were constructed by means of the FEFF 8.1 program,[24,25] to obtain ab initio calculated amplitude $f_{eff}(k)_i$, phase shift $\phi_{ij}(k)$, and mean free path $\lambda(k)$ functions (eq 1). The FEFF input file was generated by means of the ATOMS program,[26] using structural information from the crystal structure of the reference compound $Cd(SCH_2CH_2NH_2)_2$, with both short and long Cd−S, Cd−N(/O), and Cd−Cd distances.[16] This compound was suitable for creating different models, making use of the fact that the scattering parameters for the nitrogen and oxygen atoms are quite similar.

$$\chi(k) = \sum_i \frac{N_i \cdot S_0^2(k)}{k \cdot R_i^2} |f_{eff}(k)|_i \exp(-2k^2\sigma_i^2) \exp[-2R_i/\lambda(k)] \sin[2kR_i + \phi_{ij}(k)] \quad (1)$$

The structural parameters for each significant contribution to the $\chi(k)$ model function were refined by least-squares methods, fitting the k^3-weighted $\chi(k)$ function to the experimental unfiltered EXAFS oscillations over the k ranges 2.4−16.0 Å^{-1}, 2.4−12.0 Å^{-1}, and 3.4−12.0 Å^{-1}, allowing the bond distance (R), disorder (Debye−Waller) parameter (σ^2), amplitude reduction factor (S_0^2), and ΔE_0 (correlated parameter for all scattering paths) to float, while the coordination number (N) was fixed. The fitting results for **2** are shown in Figure 3 and Figures S-4 and S-5 (Supporting Information) and Table 2 and Table S-3 (Supporting Information). In models **I** and **VIIIa** (Table 2), the estimated error limits for the refined Cd−S and Cd−O bond distances are ±0.02 Å and ±0.04 Å and for the corresponding disorder parameters are ±0.001 and ±0.003−0.005 Å^2, respectively, including effects of systematic deviations.

Results

Vibrational Spectroscopy. The vibrational bands attributed to the cadmium(II) complexes of **1** and **2** are almost identical (Figure 1 and Table S-1, Supporting Information). For **2**, the Raman bands at 932 cm^{-1} (symmetric ClO_4^-

(15) Petrova, R.; Bakardjieva, S.; Todorov, T. *Z. Kristallogr.* **2000**, *215*, 118.
(16) Bharara, M. S.; Kim, C. H.; Parkin, S.; Atwood, D. A. *Polyhedron* **2005**, *24*, 865–871.
(17) Nardelli, M.; Gasparri, G. F.; Boldrini, P. *Acta Crystallogr.* **1965**, *18*, 618–623.
(18) Ye, C.; Fu, R.; Hu, J.; Hu, L.; Ding, S. *Magn. Reson. Chem.* **1993**, *31*, 699–704.
(19) Mennitt, P. G.; Shatlock, M. P.; Bartsuka, V. J.; Maciel, G. E. *J. Phys. Chem.* **1981**, *85*, 2087–2091.
(20) Herzfeld, J.; Berger, A. E. *J. Chem. Phys.* **1980**, *73*, 6021–6030.
(21) Eichele, K.; Wasylishen, R. E. *HBA*, v. 1.5; University of Alberta: Edmonton, Canada; Universität Tübingen: Tübingen, Germany, 2006.
(22) Eichele, K.; Wasylishen, R. E. *WSolids*, v. 1.17.30; University of Alberta: Edmonton, Canada, 2001.
(23) Ressler, T. *J. Synchrotron Radiat.* **1998**, *5*, 118–122.
(24) Zabinsky, S. I.; Rehr, J. J.; Ankudinov, A.; Albers, R. C.; Eller, M. J. *Phys. Rev. B* **1995**, *52*, 2995–3009.
(25) Ankudinov, A. L.; Rehr, J. J. *Phys. Rev. B* **1997**, *56*, R1712−R1716.
(26) Ravel, B. *J. Synchrotron Radiat.* **2001**, *8*, 314−316.

stretching), 627 cm^{-1} (antisymmetric ClO_4^- bending), and 460 cm^{-1} (symmetric ClO_4^- bending), as well as the IR absorption bands at 1117 and 627 cm^{-1}, belong to the ClO_4^- ion (Figure 1 and Table S-2, Supporting Information).[27] To accommodate ClO_4^- in **2**, a positively charged counterion is required, as the $Cd(HCys)_2$ complex itself is neutral. Subtractions of the IR and Raman spectra of **1** from **2** (see Table S-2, Supporting Information) reveal some remaining spectral features besides those of the perchlorate anion. A strong IR band at 3210 cm^{-1} and minor residues at 1581 cm^{-1} and 1040 cm^{-1} can be assigned to the ν_1, ν_4, and ν_2 fundamental modes of the H_3O^+ ion, respectively. For solid hydronium perchlorate, the Raman bands at 3285, 1571, and 1175 cm^{-1}, assigned as the ν_1, ν_4, and ν_2 modes of the pyramidal H_3O^+ ion,[28] are in fairly good agreement with our observations. Hence, the main differences between the spectra of **1** and **2** are due to the presence of perchlorate and H_3O^+ ions in **2**, for which the chemical composition $\{Cd(HCys)_2 \cdot H_2O\}_2 \cdot H_3O^+ClO_4^-$, with one protonated water molecule, is proposed. In the difference Raman spectrum between **2** and **1**, a very weak Raman band at 1736 cm^{-1} indicates hydrogen bonding between carboxylate and H_3O^+ ions in **2** (Table S-2, Supporting Information).[29]

The cysteine molecule has three potential coordination sites: the thiol (−SH), carboxylate, and amine groups. The cysteine S−H stretching band at 2554 cm^{-1} disappeared in the spectra of **1** and **2** (Table S-1 and Figure S-1, Supporting Information), indicating that all thiol groups are deprotonated and coordinated as thiolates to the cadmium(II) ion. The downshift in the Raman C−S stretching band from 694 cm^{-1} to 681−683 cm^{-1} (Figure 1) indicates that the coordination weakens the C−S bond.[30] The strong bands at 1620−1624 cm^{-1} and 1490−1491 cm^{-1} in the IR spectra of **1** and **2**, assigned as antisymmetrical and symmetrical NH_3^+ deformation modes, respectively,[31] show that the amine group is protonated ($-NH_3^+$) and, therefore, not binding to the cadmium(II) ion (Table S-1, Supporting Information). The asymmetric and symmetric COO^- stretching modes of cysteine at 1587 and 1394 cm^{-1} [29] shift slightly in the IR spectra of **1** and **2** to $\nu_a(COO^-) = 1574-1575$ cm^{-1} and $\nu_s(COO^-) = 1398-1400$ cm^{-1}.

^{13}C, ^{113}Cd NMR Spectroscopy. ^{13}C NMR spectra of solid cysteine and the compounds **1** and **2** are shown in Figure 2. The three sharp peaks in the spectrum of cysteine at $\delta(^{13}C) = 27.8$, 55.7, and 173.2 ppm are ascribed to its $C_\beta(-S)$, C_α, and carboxylate groups (COO^-), respectively.[18] The spectra of the cadmium(II) cysteinate complexes **1** and **2** appear very similar; the three peaks are broader than those of solid cysteine and are shifted downfield by 0.4, 0.8, and 0.7 ppm, respectively. These changes are associated with either the interaction of the cysteine functional groups with cadmium(II) ions ($-S^-$, $-COO^-$) or hydrogen bonding with the hydrating water molecules ($-COO^-$, NH_3^+) or H_3O^+ ions ($-COO^-$).

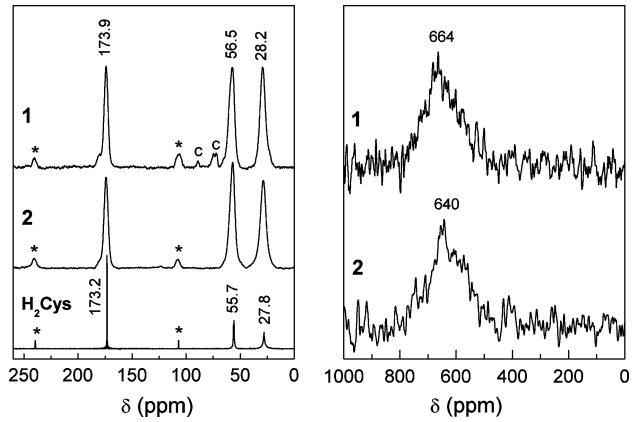

Figure 2. (Left) ^{13}C NMR spectra of the $Cd(HCys)_2 \cdot H_2O$ (**1**) and $\{Cd(HCys)_2 \cdot H_2O\}_2 \cdot H_3O^+ClO_4^-$ (**2**) amorphous solids compared with the spectrum of crystalline cysteine. The signals marked with * are spinning sidebands, and those with "c" are due to the cotton used to pack the sample (see Figure S-2, Supporting Information). (Right) ^{113}Cd NMR spectra of **1** and **2**.

Table 1. ^{113}Cd Chemical Shifts Reported for Cadmium(II)−Thiolates with CdS_xO_y Coordination Sites[a]

coordination	chemical shift (δ, ppm)	reference
CdS_4 (mononuclear)	650, 680, 704−751	35, 57−60
CdS_4 (multinuclear)	600−707	34, 53, 61
CdS_3 (peptides)	572, 684−690	62−65
CdS_3 (s)	590 (577[b]), 613, 668	66, 67
CdS_3O (peptides)	560−645	62−64, 68
CdS_3O_2 (s)	393, 400	69
CdS_3O_3 (s)	391−409	39
CdS_4O (s)	481−507	39
CdS_4O_2 (s)	245	this work
CdS_2O_4 (s)	98, 123	14, this work
CdS_2O_2	76, 144, 191	70, 71

[a] s = solid; for solids, δ_{iso} = isotropic shifts are reported; [b] In $CDCl_3$ and DMF.

The ^{113}Cd NMR spectra of the amorphous solid compounds **1** and **2** are also similar, showing a single broad peak with its maximum in the 640−664 ppm region. The broadness of these peaks is attributed to the amorphous nature of the compounds: a range of isotropic shift (δ_{iso}) values are obtained for each sample. This is consistent with the broad ^{13}C peaks obtained (Figure 2). The chemical shifts (isotropic shifts for solids; δ_{iso}) for several types of CdS_xO_y coordination sites that have been reported are shown in Table 1. Given the broad peaks obtained for **1** and **2**, the exact values for

(27) Nebgen, J. W.; McElroy, A. D.; Klodowski, H. F. *Inorg. Chem.* **1965**, *4*, 1796–1799.
(28) Taylor, R. C.; Vidale, G. L. *J. Am. Chem. Soc.* **1956**, *78*, 5999–6002.
(29) Sze, Y. K.; Davis, A. R.; Neville, G. A. *Inorg. Chem.* **1975**, *14*, 1969–1974.
(30) Susi, H.; Byler, D. M.; Gerasimowics, W. V. *J. Mol. Struct.* **1983**, *102*, 63–79.
(31) Neville, G. A.; Drakenberg, T. *Can. J. Chem.* **1974**, *52*, 616–622.
(32) Pickering, I. J.; Prince, R. C.; George, G. N.; Rauser, W. E.; Wickramasinghe, W. A.; Watson, A. A.; Dameron, C. T.; Dance, I. G.; Fairlie, D. P.; Salt, D. E. *Biochim. Biophys. Acta* **1999**, *1429*, 351–364.
(33) Isaure, M-P.; Fayard, B.; Sarret, G.; Pairis, S.; Bourguignon, J. *Spectrochim. Acta, Part B* **2006**, *61*, 1242–1252.
(34) Oz, G.; Pountney, D. L.; Armitage, I. M. *Biochem. Cell Biol.* **1998**, *76*, 223–234.
(35) Bobsein, B. R.; Myers, R. J. *J. Am. Chem. Soc.* **1980**, *102*, 2454–2455.
(36) Engeseth, H. R.; McMillin, D. R.; Otvos, J. D. *J. Biol. Chem.* **1984**, *259*, 4822–4826.
(37) Meijers, R.; Morris, R. J.; Adolph, H. W.; Merli, A.; Lamzin, V. S.; Cedergren-Zeppezauer, E. S. *J. Biol. Chem.* **2001**, *276*, 9316–9321.
(38) Bobsein, B. R.; Myers, R. J. *J. Biol. Chem.* **1981**, *256*, 5313–5316.
(39) Jalilehvand, F.; Leung, B. O.; Mah, V. *Inorg. Chem.* Submitted.

Table 2. Alternative Models Used for EXAFS Curve-Fitting of $\{Cd(HCys)_2 \cdot H_2O\}_2 \cdot H_3O^+ClO_4^-$ (**2**) in the k Range 2.4−16.1 Å^{-1} (see Figure S-4, Supporting Information)[a]

		Cd−S			Cd−O					
model	coordination model	N	R (Å)	σ^2 (Å^2)	N	R (Å)	σ^2 (Å^2)	S_0^2 [b]	ΔE_0	R[c]
I	CdS_4	4 *f*	2.515	0.0088				0.85	−1.6	24.0
II	CdS_3	3 *f*	2.515	0.0088				1.13	−1.6	24.0
III	CdS_3S'	1 *f*	2.403	0.0082				0.92	−3.4	22.1
		3 *f*	2.523	0.0066						
IV	$CdS_2S'_2$	2 *f*	2.453	0.0105				0.91	−3.6	22.2
		2 *f*	2.531	0.0058						
V	CdS_2S'	1 *f*	2.423	0.0094				1.22	−3.5	22.1
		2 *f*	2.526	0.0064						
VI	CdS_4O	4 *f*	2.523	0.0072	1 *f*	2.257	0.0066	0.68	−0.7	21.6
VII	CdS_4O_2	4 *f*	2.528	0.0070	2 *f*	2.300	0.0106	0.62	0.6	21.5
VIIIa	CdS_3O	3 *f*	2.525	0.0070	1 *f*	2.273	0.0079	0.87	−0.2	21.5
VIIIb		3 *f*	2.528	0.0074	2.1	2.350	0.0166	0.85 *f*	1.5	21.4
IX	CdS_3O_2	3 *f*	2.525	0.0087	2 *f*	2.434	0.0298	1.10	1.0	21.0
X	CdS_3O_3	3 *f*	2.527	0.0089	3 *f*	2.466	0.0371	1.14	1.4	19.9
XI	CdS_2O_2	2 *f*	2.527	0.0089	2 *f*	2.466	0.0371	1.71	1.4	19.9
XII	CdS_2O_4	2 *f*	2.542	0.0048	4 *f*	2.347	0.0100	0.70	4.0	26.2

[a] N = coordination number; f = fixed; [b] For model **VIII b**, the S_0^2 was fixed at 0.85, a value obtained from EXAFS fitting of standard complexes.[39] [c] The residual (%) from the least-squares curve fitting is defined as $\{[\sum_{i=1}^{N}|y_{exp}(i) - y_{theo}(i)|]/[\sum_{i=1}^{N}|y_{exp}(i)|]\} \times 100$, where y_{exp} and y_{theo} are experimental and theoretical data points, respectively.

δ_{iso} are uncertain, but the isotropic values fall in the 500−700 ppm range, which is a region characteristic for CdS_4, CdS_3, CdS_3O, and CdS_4O coordination geometries (see Table 1). The vibrational spectra showed protonated amine groups in both **1** and **2**, and therefore, CdS_xN_y coordination is not possible in these compounds.

Cd K-Edge EXAFS Spectroscopy. To further examine **1** and **2**, their Cd K-edge EXAFS spectra were measured. The complete overlap of the two EXAFS oscillations (Figure S-3, Supporting Information) indicated the same local structure around the cadmium(II) ions in both solids. Because of the similarity of the spectra, only the results for compound **2** are discussed. Different data k ranges (2.4−16.1 Å^{-1}, 2.4−12.0 Å^{-1}, and 3.5−12.0 Å^{-1}) and several coordination models were used for the least-squares model fitting (Table 2, Tables S-3a and S-3b and Figures S-4 and S-5, Supporting Information). For all models in different data k ranges, the average Cd−S bond distance of 2.52 ± 0.02 Å consistently emerged (Table 2 and Tables S-3a and S-3b, Supporting Information). The average Cd−O distance for CdS_3O, CdS_4O, and CdS_4O_2 models (**VI**−**VIIIa**) varied between 2.22 and 2.30 Å using different k ranges in the refinements. Within each data k range, the differences in the residuals were not conclusive. Figure 3 shows the results for the CdS_3O model (**VIIIa** in Table 2), including the separate contributions of the Cd−S and Cd−O scattering paths.

A small peak at ∼3.5 Å (not corrected for the phase shift) was observed in the Fourier transform (FT) of the EXAFS spectra of **1** and **2** (Figure 3). Attempts to include a Cd−Cd scattering path in models **I** and **VIIIa** were unsuccessful in reproducing the feature properly, showing a contribution of less than 2% for this path. For oligomeric complexes with a double thiolate bridge such as bis(cysteaminate)cadmium(II) $[Cd(SCH_2CH_2NH_2)_2]$, the well-defined Cd···Cd distance at 3.64 Å gives rise to a distinct FT peak (Figure S-6, Supporting Information). However, for the cadmium adamantane cage structure, $(Et_3NH)_4[S_4Cd_{10}(SPh)_{16}]$, with single thiolate bridges between the cadmium(II) ions, no peak could be discerned for Cd···Cd interactions between 3 and 4 Å (Figure S-6a, Supporting Information).

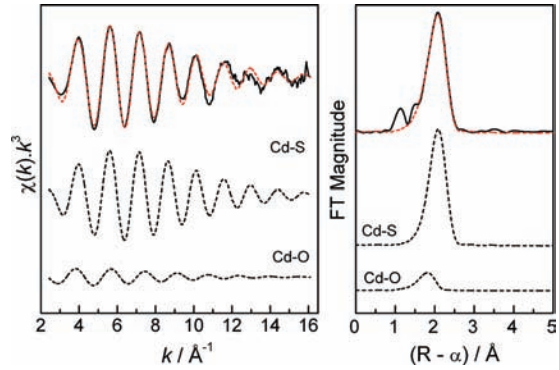

Figure 3. Least-squares curve-fitting of the k^3-weighted EXAFS spectrum of **2** for a CdS_3O model (**VIIIa**, Table 2) and the corresponding Fourier transforms, with separate Cd−S and Cd−O contributions.

Cd L_3-Edge XANES Spectroscopy. Cd L_3-edge XANES spectra have been proposed to be sensitive to the local structure and type of the coordinating atoms in cadmium(II) complexes.[32,33] Therefore, we prepared and measured the Cd L_3-edge XANES spectra of several crystalline $CdS_x(O/N)_y$ complexes with different coordination geometries (see the Experimental Section and Figure S-7, Supporting Information), for comparisons with the indistinguishable spectra of **1** and **2** (Figure 4). The distinct pre-edge peak at 3539.1 eV in the spectrum of $Cd(ClO_4)_2 \cdot 6H_2O$ (CdO_6 model) gradually blends into the absorption edge of the spectra of the standard compounds used as CdS_2O_4 (I and II), CdS_3O_3, CdS_6, CdS_3O, and CdS_2N_2 models and finally disappears in the CdS_3N_2 and CdS_4 spectra. This pre-edge feature is due to a transition from Cd $2p_{3/2}$ to unoccupied molecular orbitals with mainly s and d character.

The Cd L_3-edge XANES spectra of **1** and **2** display two shoulders at 3539.1 and 3541.3 eV, which become more distinct in the second derivative (see Figure 4). The shapes of the absorption edge features for **1** and **2** and their corresponding second derivatives appear intermediate to

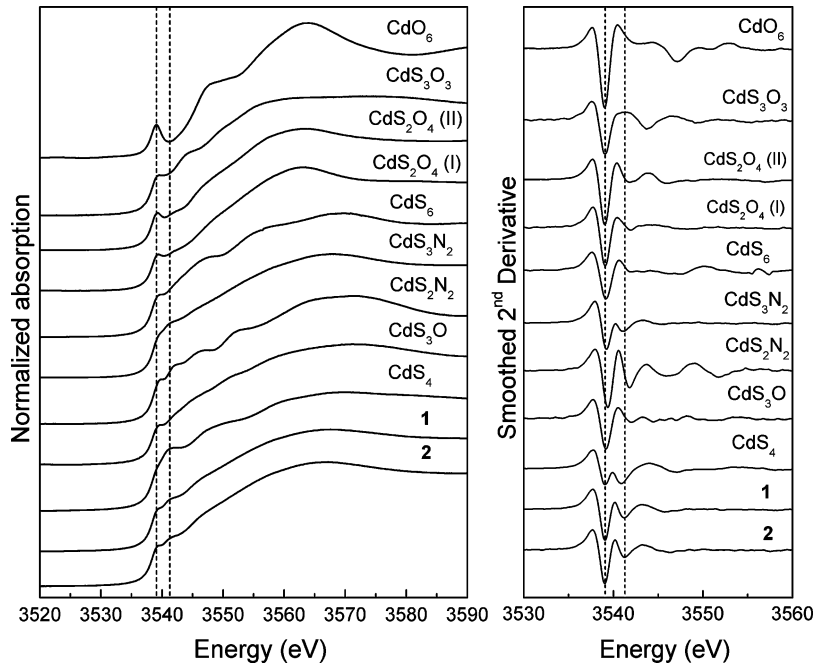

Figure 4. Cd L_3-edge XANES spectra and the corresponding smoothed second derivatives of **1** and **2**, compared with those of crystalline $CdS_x(N/O)_y$ complexes used as coordination models (see Figure S-7, Supporting Information). Dashed lines are at 3539.1 and 3541.3 eV.

those of the CdS_3O and CdS_3N_2 standards. Since the scattering parameters for the nitrogen and oxygen atoms are quite similar, the CdS_3N_2 model may represent the CdS_3O_2 configuration as well.

Discussion

The compositions of the two solid compounds obtained through the reactions of cysteine with $Cd(CH_3COO)_2 \cdot 2H_2O$ or $Cd(ClO_4)_2 \cdot 6H_2O$ were characterized as $Cd(HCys)_2 \cdot H_2O$ (**1**) (precipitated at pH = 2.7) and $\{Cd(HCys)_2 \cdot H_2O\}_2 \cdot H_3O^+ClO_4^-$ (**2**) (precipitated at pH = 1.6), respectively, based on C, N, and H elemental analyses and thermal gravimetric and IR/Raman measurements. The similarity of the Cd K-edge EXAFS, Cd L_3-edge XANES, and ^{13}C NMR spectra of **1** and **2** and the comparable ^{113}Cd NMR spectra showed closely related structures for the cadmium(II) cysteine complexes in **1** and **2**. The different composition of the cadmium(II)−cysteinate compound **2** seems to be connected to the low pH value at which it precipitated. A similar inclusion of acid in a crystal structure has been reported for the Hg(II) cysteinate complex, $Hg(HCys)_2 \cdot HCl \cdot 1/2H_2O$, prepared by reacting cysteine and $HgCl_2$.[31]

The broad signals obtained from the solid-state ^{113}Cd NMR spectra of the amorphous compounds **1** and **2** (span in the 500−700 ppm range) with maxima at ∼650 ppm (Figure 2) appear in a region characteristic for CdS_4 (especially in single-bridged multinuclear cadmium(II)−tetrathiolates, as in Cd(II) loaded metallothionein 600−680 ppm),[34] CdS_3, CdS_3O, and CdS_4O coordination geometries (see Table 1). For a NMR spectrum of a powder sample, the isotropic chemical shift is not necessarily the point of maximum intensity in the spectrum: the line shape one obtains depends on the magnitudes of the principal components (δ_{11}, δ_{22}, and δ_{33}) of the chemical shift tensor that describes the anisotropic magnetic shielding; this in turn depends on molecular properties and symmetry. This is clear from the ^{113}Cd NMR spectrum of the $Cd(tu)_2(NO_3)_2$ complex (CdS_2O_4), where the peak maximum is at ∼280 ppm, while δ_{iso} = 123 ppm (Figure S-8, Supporting Information).

The ^{113}Cd NMR spectra of **1** and **2** look very different from that previously reported for the dehydrated $Cd(HCys)_2$ solid compound, which showed narrow peaks within the ∼180−620 ppm region with a δ_{iso} value of 402 ppm, and was attributed to a chain structure with CdS_4O_2 units (Scheme 1, left). Such narrow bands are not normally consistent with an amorphous solid, and Barrie et al. interpreted the spectrum as indicating a "high degree of local order at the cadmium site".[9] Also, the assignment to a polymeric chain with CdS_4O_2 units seems doubtful for a dehydrated $Cd(HCys)_2$ compound. The only similar polymeric structure that we could find in the crystal structure database was that of crystalline $[Cd(tu)_2(HCOO)_2]$ (tu = thiourea), where thiourea acts as a bridging ligand between the cadmium(II) ions, with two sets of Cd−S distances of 2.709 and 2.740 Å and a Cd−O distance of 2.277 Å to the formate ions.[17] We measured the solid-state ^{113}Cd NMR spectrum of this complex (Figure S-9, Supporting Information) and found the isotropic chemical shift δ_{iso} = 245 ppm. To the best of our knowledge, this is the first ^{113}Cd chemical shift reported for a complex with CdS_4O_2 geometry, which is not consistent with the proposed assignment of the δ_{iso} value of 402 ppm for the dehydrated $Cd(HCys)_2$ solid compound to CdS_4O_2 coordination geometry.

The distances to the different types of atoms coordinated to the cadmium(II) ion are essential when discussing the structures of **1** and **2**. EXAFS spectroscopy provides such information for the local structure around the central absorbing atom. Since the protonated amine groups of the cysteine

Table 3. Survey of a Series of Cadmium(II) Complexes with S-Donor Ligands (distances are in ångstroms; from CSD version 5.29, Nov 2007; see Tables S-5 and S-6 in Supporting Information for details)

coordination	No. of crystal structures	Cd−S distance range	Cd−S average distance	Cd−(O/N) distance range	Cd−(O/N) average distance
CdS_3	4	2.376−2.582	2.446		
CdS_4 (mononuclear)	5	2.515−2.554	2.531		
CdS_3O	3	2.493−2.573	2.527	2.108−2.308	2.240
CdS_3N	1	2.405−2.588	2.522	2.207	2.207
CdS_2N_2	10	2.417−2.560	2.473	2.226−2.342	2.288
CdS_2O_2	2	2.634−2.767	2.701	2.102−2.121	2.112
CdS_2O_3	2	2.460−2.529	2.494	2.258−2.610	2.392
CdS_3O_2	1	2.508−2.870	2.522 (2.637)[a]	2.221−2.374	2.297
CdS_3N_2	5	2.454−3.109	2.551 (2.622)[a]	2.308−2.477	2.386
CdS_3O_3	2	2.533−2.602	2.560	2.291−2.752	2.550
CdS_2O_4	7	2.497−2.647	2.557	2.266−2.794	2.434
CdS_4O_2	3	2.646−2.740	2.683	2.277−2.470	2.385
CdS_4N_2	3	2.543−3.038	2.664 (2.716)[a]	2.331−2.479	2.394

[a] Average obtained by including longer, bridging Cd−S distances.

ligands in **1** and **2** are not able to coordinate to the cadmium(II) ion, we restricted our evaluation to CdS_xO_y coordination models. Several structural models, including CdS_4, CdS_3, CdS_3O, CdS_4O, CdS_3O_2, CdS_3O_3, CdS_2O_2, CdS_4O_2, and CdS_2O_4, were used for least-squares curve-fitting to the k^3-weighted EXAFS spectra of **1** and **2** in different k ranges: k = 2.4−16.1, 2.4−12.0, and 3.5−12.0 Å^{-1}. Almost all models tested were able to provide good fits in both k and r space (Figures S-4 and S-5, Supporting Information) because of the dominating backscattering from the sulfur atoms. The average Cd−S bond distance obtained from all model fittings was consistently 2.52 ± 0.02 Å (Table 2 and Tables S-3a and S-3b, Supporting Information). The minor Cd−O contribution was more difficult to analyze because of the dominating backscattering from the sulfur atoms. For the CdS_3O, CdS_4O, and CdS_4O_2 models (**VI**−**VIIIa**), the average Cd−O distance and corresponding disorder parameter varied between 2.22 and 2.30 Å and 0.005 and 0.013 Å^2, when fitting the EXAFS oscillation at different k ranges. The CdS_4O (**VI**) and CdS_4O_2 (**VII**) models resulted in unreasonably small amplitude reduction factors (S_0^2) of 0.6−0.7. For the CdS_3O_2, CdS_3O_3, CdS_2O_2, and CdS_2O_4 models (**IX**−**XII**), the Cd−O distance fluctuated drastically between 2.28 and 2.48 Å by changing the fitting k range and was accompanied by unstable disorder parameters (σ^2 from 0.008 to 0.05 Å^2) and S_0^2 values. Those extreme changes in Cd−O distances, σ^2(Cd−O), and S_0^2 values indicated that the **IX**−**XII** models did not properly represent the Cd(II) sites in **1** and **2**.

The main conclusion derived from the above EXAFS data analyses is that the mean Cd−S distance is 2.52 ± 0.02 Å for **1** and **2**. To identify the dominating type of coordination environment, the mean Cd−S bond distance obtained from the EXAFS spectra was used for comparisons with those in structurally known cadmium(II) complexes with S-donor ligands, aided by the broad signal observed in their solid-state ^{113}Cd NMR spectra in the 500−700 ppm region, with peak maxima around 650 ppm. Such comparisons are more likely to provide reliable information on the coordination geometry of the cadmium(II) ion in **1** and **2** than the coordination numbers obtained from EXAFS, which have low accuracy because of the correlation with other parameters affecting the amplitude of an EXAFS oscillation, that is, the amplitude reduction factor (S_0^2) and the Debye−Waller (disorder) parameter (σ^2).

Table 3 provides ranges and average values of the Cd−S and Cd−(O/N) bond distances in a series of crystalline cadmium(II) complexes with S-donor ligands (structural details are provided in Tables S-5 and S-6 in the Supporting Information). As shown in Table S-6, the nature and denticity of the ligands strongly influence the distribution of metal−ligand bond distances. Some coordination figures have only been found with S ligands other than thiolates, such as thiourea. For some crystal structures, for example, dinuclear complexes with CdS_3O_2, CdS_3N_2, or CdS_4N_2 coordination, shown in Table 3 and Table S-5, the distribution of Cd−S bond distances is wide since the S-donor ligands act as both terminal and bridging groups. In such cases, two mean values of the Cd−S distances have been provided, with and without accounting for the contribution from the long Cd−S distances. When comparing the average of a range of distances obtained from EXAFS data with those determined by crystallography, care should be taken, as shorter distances generally have a higher contribution to the EXAFS oscillation (due to the 1/R factor in eq 1, and often lower σ^2 values).

Possible CdS_xO_y Coordination Sites for the Amorphous Solids 1 and 2.

CdS_2O_2 Coordination. The ^{113}Cd NMR chemical shifts reported for CdS_2O_2 coordination in Table 2 are obtained for S-donor ligands other than thiolates and may not be fully comparable with those of **1** and **2**, which span 500−700 ppm. A more appropriate estimate of the expected ^{113}Cd chemical shift for CdS_2O_2 coordination with thiolates can be obtained by considering the ^{113}Cd chemical shifts found for cadmium-substituted horse liver alcohol dehydrogenase (LADH), and its binary complex with nicotinamide adenine dinucleotide, LADH−NAD(H). In cadmium(II)−LADH, the Cd(II) ion occupies a CdS_2NO coordination site, $\delta(^{113}Cd)$ = 483 ppm, where it is surrounded by two cysteine thiolates, one imidazole nitrogen, and one water molecule.[35,36] For the cadmium(II)-substituted LADH−NAD(H), for which the 1-Å-resolution X-ray structure revealed a CdS_2NO_2 coordi-

nation site,[37] the ^{113}Cd NMR resonance becomes shielded (442−443 ppm) relative to that of cadmium(II)−LADH (483 ppm).[38] Nitrogen is more deshielding than oxygen, and removing the nitrogen ligand from a CdS_2NO_2 site would further shift the ^{113}Cd signal upfield. Therefore, for a cadmium(II) thiolate complex with a stable CdS_2O_2 coordination environment, a ^{113}Cd chemical shift of ∼400 ppm would be expected, which still is shielded relative to the broad 500−700 ppm signal of **1** and **2**. Moreover, using this model for EXAFS curve-fitting of **1** and **2** resulted in very high values of S_0^2 and disorder parameters for the Cd−O scattering path (**XI**, Table 2). Hence, CdS_2O_2 coordination is not likely for the cadmium(II) site in **1** and **2**.

CdS_2O_3 Coordination. For this type of coordination, the ^{113}Cd chemical shift is expected to be more shielded than for CdS_3O_2 coordination (≪400 ppm, Table 1), as an oxygen ligand atom is more shielding than sulfur. Therefore, such a coordination environment is unlikely in **1** and **2**, even though the average Cd−S bond distance for CdS_2O_3 coordination, ∼2.49 Å (Table 3), is close to the mean Cd−S distance 2.52 ± 0.02 Å obtained for **1** and **2**.

CdS_2O_4 Coordinations. Also, the mean Cd−S bond distance for this type of coordination (∼2.56 Å) is fairly close to that obtained for **1** and **2**. EXAFS curve fitting using this model over the k range = 2.4−16.1 Å^{-1} gave reasonable values for the refined parameters (**XII**, Table 2). However, reducing the fitting range to 2.4−12 Å^{-1} and 3.5−12 Å^{-1} resulted in very small (0.61), or very large, S_0^2 values (1.55), respectively, indicating an inadequate model. The reported ^{113}Cd chemical shift values (∼100 ppm; Table 1) for CdS_2O_4 compounds (S-donor ligand = thiourea, tetramethylthiourea) are considerably more shielded than the broad ^{113}Cd NMR signals of **1** and **2** (∼450−780 ppm). Therefore, on the basis of the combined NMR and EXAFS results, CdS_2O_4 coordination is not expected in **1** and **2**.

CdS_3 Coordination. The average Cd−S bond distance for cadmium(II) complexes with CdS_3 coordination is ∼2.45 Å (Table 3), which is considerably shorter than the mean Cd−S distance of 2.52 ± 0.02 Å for **1** and **2**. Therefore, this type of coordination mode is unlikely, even though the reported ^{113}Cd chemical shift for CdS_3 coordination falls within the broad ^{113}Cd NMR signals of **1** and **2**.

CdS_3O_2 and CdS_3O_3 Coordination. The average Cd−S bond distances for CdS_3O_2 and CdS_3O_3 coordination, ∼2.52 and 2.56 Å, respectively, do not differ significantly from the mean Cd−S distance of 2.52 ± 0.02 Å for **1** and **2**. Least-squares curve-fitting of the EXAFS oscillations for **1** and **2** using these models at different k ranges showed very large disorder parameters (σ^2) for the Cd−O scattering path, as well as highly fluctuating Cd−O bond distances and S_0^2 values (**IX** and **X** in Table 2 and Table S-3a,b, Supporting Information). Fixing the coordination number $N_{Cd-S} = 3$ and keeping S_0^2 at 0.85, a value obtained from EXAFS fitting of standard complexes,[39] resulted in refined N_{Cd-O} values between 0.8 and 2.1 (depending on the k-fitting range), R_{Cd-O} = 2.24−2.35 Å, and σ^2 = 0.006−0.016 Å^2 (model **VIIIb**, Table 2 and Table S-3a,b, Supporting Information). The reported chemical shifts for these coordination geometries are about 400 ppm, which is rather shielded relative to the broad ^{113}Cd NMR signals of **1** and **2**. Since both NMR and EXAFS spectra provide average values for all possible cadmium(II) ion sites in the sample, a minor amount of such coordination geometries in **1** and **2** cannot be ruled out.

CdS_4O Coordination. The decanuclear cadmium complex of the compound $[Cd_{10}(SCH_2CH_2OH)_{16}](ClO_4)_4 \cdot 8H_2O$ has CdS_4O coordination sites with average Cd−S and Cd−O bond distances of 2.594 and 2.410 Å, respectively.[40] The corresponding mean distances obtained when using this type of model (**VI**) for EXAFS fitting—Cd−S, 2.52 ± 0.02 Å and Cd−O, 2.22−2.26 Å (Table 2 and Table S-3a,b, Supporting Information)—are considerably shorter. The reported ^{113}Cd chemical shift of 481−507 ppm falls within the region where the ^{113}Cd NMR signals for **1** and **2** appear (500−700 ppm). Therefore, a minor amount of cadmium(II) complexes with such coordination is possible in **1** and **2**.

CdS_4O_2 Coordination. The proposed structure by Barrie et al. for a dehydrated $Cd(HCys)_2$ compound has such a coordination environment (Figure 1, left).[9] The solid-state ^{113}Cd NMR isotropic shift of 245 ppm for the $[Cd(tu)_2(HCOO)_2]$ complex with CdS_4O_2 coordination (Figure S-9, Supporting Information) shows considerable shielding relative to the ^{113}Cd NMR signals of **1** and **2**. Also, the average crystallographic Cd−S bond distance in CdS_4O_2 complexes (∼2.68 Å; Table 3) is much longer than the mean Cd−S distance of 2.52 ± 0.02 Å, obtained for **1** and **2**. EXAFS curve-fitting of **1** and **2** using this model (**VII**) resulted in a fairly constant Cd−O distance (2.26−2.30 Å) but an unrealistic, small S_0^2 value (0.6). Therefore, CdS_4O_2 coordination, with its high shielding and long mean crystallographic Cd−S distance, is unlikely for the cadmium(II) ions in **1** and **2**.

CdS_4 and CdS_3O Coordination. We have recently reported the Cd L_3-edge spectra of a series of cadmium(II) cysteine solutions (pH 11.0), with an increasing excess of cysteine. The solutions with molar ratios $C_{H_2Cys}/C_{Cd(II)}$ of 15−20 and ^{113}Cd chemical shifts of 654−658 ppm were found to contain predominantly $[Cd(Cys)_4]^{6-}$ (CdS_4) complexes, with very similar features in the second derivative of their Cd L_3-edge spectra to those of the standard CdS_4 compound.[39] However, the different relative sizes of the corresponding two main features for **1** and **2** (Figure 4) to some extent resemble those of the CdS_3O standard model compound and indicate that CdS_4 cannot be the only type of coordination occurring in **1** and **2**.

Attempts to describe the k^3-weighted EXAFS spectra of **1** and **2** with a model including only Cd−S backscattering, that is, as for CdS_4 coordination, showed a relatively poor fit at high k values (k > 10.5 Å^{-1}) and r ∼ 1.5 Å, when fitting the data in the k range 2.4−12.0 Å^{-1} (model **I**, Figure S-5, Supporting Information), while including Cd−O in CdS_3O coordination (**VIIIa**) improved the fitting residual. Both models resulted in average Cd−S distances of 2.52 ±

(40) Lacelle, S.; Stevens, W. C.; Kurtz, D. M.; Richardson, J. W.; Jacobson, R. A. *Inorg. Chem.* **1984**, *23*, 930–935.

Table 4. Assignment of Far-Infrared and Raman Bands (cm^{-1}) of **1** and **2** (see Figure 5)

$Cd(HCys)_2 \cdot H_2O$ (**1**)		$\{Cd(HCys)_2 \cdot H_2O\}_2 \cdot H_3O^+ClO_4^-$ (**2**)		
IR	Raman	IR	Raman	assignment
687 m, w	683 s	670 w	681 vs	νCS, δCO_2
622 w	629 w	*a*	*a*	ωCO_2
		625 vs	627 s	$\nu_4[ClO_4]^-$
531 vs	521 m	531 vs	531 w, m	ρCO_2, δNCC
464 w, sh	467 m, sh	464 w	*a*	δNCC
			463/458m	$\nu_2[ClO_4]^-$
420 vw	420 vvw	420 vvw	420 vvw	$\tau NH_3^+/\delta$NCC
365 s	372 vw	365 s	~360 vvw	δCCS
	275 s		278 s	ν_sCdS terminal
(~275)		(~278)		ν_aCdS terminal[b]
255 s, sh		~250 m, b		ν_aCdS bridging[c]
	239 w, sh		244 m, sh	ν_sCdS bridging
221 vs, b		228 vs, b		ν_aCdS bridging
150 m, sh		164 m, sh		δOCdO, δOCdS

[a] Overlapping with $[ClO_4]^-$ bands. [b] Estimated values close to ν_sCdS Raman features. [c] An alternative assignment of these bands to the Cd−O stretching of weakly coordinated carboxyl oxygen.

0.02 Å, which is close to that of the crystalline cadmium(II) complexes with tetrahedral CdS_4 (mononuclear) and CdS_3O coordination ($Cd-S_{ave}$ = 2.53 Å) in Table 3. Among all CdS_xO_y models used for the EXAFS curve-fitting (**VI**−**XII**), only the CdS_3O (model **VIIIa**) consistently yielded plausible sets of refined parameters over different fitting *k* ranges. The Cd−O distance obtained values in the range 2.24−2.27 Å, compatible with that observed for CdS_3O crystalline compounds (Table 3), with a corresponding reasonable disorder parameter σ^2 = 0.007−0.01 $Å^2$. While the amplitude reduction factor (S_0^2 = 0.8−0.9) became realistic for both models, the relatively high disorder parameter for the Cd−S scattering pathway in model **I** (σ^2 = 0.008(1) $Å^2$) indicated a fairly large distribution of the Cd−S distances. An attempt to resolve the Cd−S distances by means of the CdS_3S' and $CdS_2S'_2$ models (**III** and **IV**, Table 2 and Table S-3a,b, Supporting Information) was not successful, leading to higher σ^2 values for the shorter Cd−S distances.

However, the Cd−S vibrational bands in the Raman and far-IR spectra can be used as a probe for terminal and bridging Cd−S bonds. A single Cd−S stretching Raman band has been observed at 269 cm^{-1} for a cadmium(II)−cysteine complex[41] and at 282 cm^{-1} for a cadmium(II)-bound zinc-finger peptide.[42] The Raman bands at 275 and 278 cm^{-1} of **1** and **2**, respectively, can similarly be attributed to symmetric stretching of the Cd−S terminal bonds (Table 4, Figure S-10, Supporting Information). The asymmetric terminal Cd−S stretching band is expected to be very close to the Raman band at 275 cm^{-1} due to an absence of vibrational coupling between the terminal Cd−S bonds, but it is difficult to locate its position in the very broad and overlapping infrared features between 300 and 150 cm^{-1} (Figure 5). The strongest IR bands for **1** and **2** in the far-IR region, at 221 and 228 cm^{-1}, respectively, are the best candidates for the bridging Cd−S antisymmetric stretching. Close to the positions of these far-IR bands, the Raman spectra exhibit shoulders at 239 and 244 cm^{-1}, which can

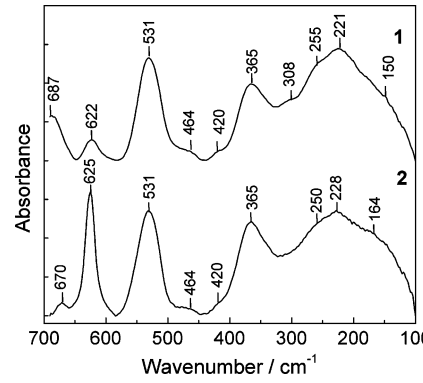

Figure 5. Far-infrared spectra of $Cd(HCys)_2 \cdot H_2O$ (**1**) and $\{Cd(HCys)_2 \cdot H_2O\}_2 \cdot H_3O^+ClO_4^-$ (**2**).

be assigned as symmetric stretches of bridging Cd−S (Table 4, Figure S-10). Beside those, the shoulders in the IR spectra for **1** and **2** at 255 and 250 cm^{-1}, respectively, can also be assigned to the antisymmetric vibrational modes of the bridging Cd−S bonds. Therefore, we propose an assignment where the higher-frequency bands at ~275 cm^{-1} belong to the stretchings of the terminal Cd−S bonds and the lower-frequency bands between 255 and 221 cm^{-1} to the stretching modes of the weaker bridging Cd−S bonds (Table 4).

A closer look at low-frequency bands (<275 cm^{-1}) in Table 4 shows that the far-IR and low-frequency Raman features do not coincide in any position, which suggests a symmetric structure close to a center of inversion in the cadmium(II) complexes in **1** and **2**. In addition to the bridging Cd−S stretching features, other skeletal modes like CS stretchings and CCS bendings also exhibit 5−10 cm^{-1} splittings between IR and Raman spectra in accordance with the mutual exclusion rule for centrosymmetry.

The possible coordination of the carboxylate oxygen atoms was probed by means of the C−O stretching bands. Generally, the carboxylate group can act as an uncoordinated anion ("ionic" form), a monodentate or bidentate chelating ligand, or as a bridging bidentate group. Several empirical correlations have been made between the coordination mode of the COO^- group and the separation between the antisymmetric and symmetric C−O stretchings, $\Delta\nu = \nu_a(COO^-) - \nu_s(COO^-)$, from IR spectra of metal acetate complexes in the anhydrous form or in aqueous solution.[43−46]

With monodentate coordination, that is, a M−O bond formed to a metal ion, the two C−O bonds of the carboxylate group are no longer equivalent, as they are in the "ionic" form for "free" COO^-. Nakamoto studied metal complexes of amino acids and observed that, generally upon coordination, $\nu_a(COO^-)$ increases and $\nu_s(COO^-)$ decreases, and that an increase in the covalent character of the M−O bond leads to more asymmetrical structure of the carboxylate group and,

(41) Faget, O. G.; Felcman, J.; Giannerini, T.; Téllez, S. C. A. *Spectochim. Acta, Part A* **2005**, *61*, 2121–2129.
(42) Vargek, M.; Zhao, X.; Lai, Z.; McLendon, G. L.; Spiro, T. G. *Inorg. Chem.* **1999**, *38*, 1372–1373.
(43) Deacon, G. B.; Phillips, R. J. *Coord. Chem. Rev.* **1980**, *33*, 227–250.
(44) Simon-Kutscher, J.; Gericke, A.; Hühnerfuss, H. *Langmuir* **1996**, *12*, 1027–1034.
(45) Tackett, J. E. *Appl. Spectrosc.* **1989**, *43*, 483–489.
(46) Nakamoto, K. *Infrared and Raman Spectra of Inorganic and Coordination Compounds*, 5th ed., Part B; John Wiley Inc.: New York, 1997; pp 59−67.

Scheme 2. A "Cyclic/Cage" Type of Structure, Such As **A**, **B**, and **C**, Is Proposed for the $Cd(HCys)_2 \cdot H_2O$ Complex in **1** and **2**, with CdS_3O and CdS_4 Coordination Entities Joined by a Single Thiolate Bridge[a]

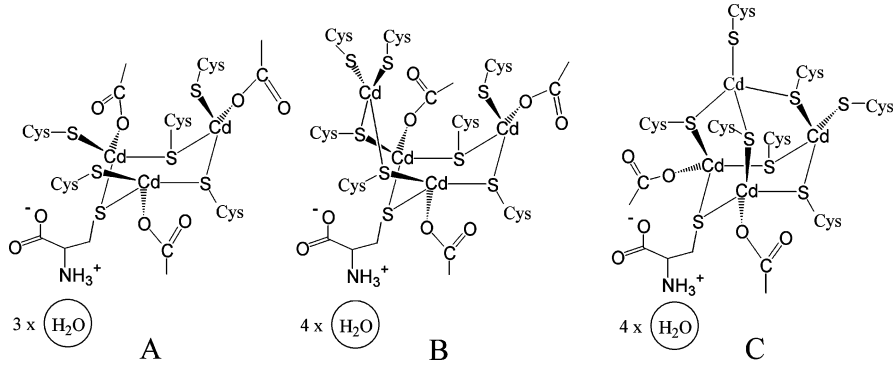

[a] Structures **A** and **B** are similar to those of the Cd_3S_9 and Cd_4S_{11} clusters in Cd_7−metallothionein.

therefore, a larger band separation ($\Delta\nu$).[46,47] This effect is sometimes counteracted by, for example, hydrogen-bond formation to the other oxygen atom. The competition of these two effects controls the shifts of the bands. Therefore, the positions of the $\nu(COO^-)$ bands for amino acid metal complexes in the solid state are not only influenced by the direct coordination to a metal ion but also by hydrogen bonding with water of crystallization, or other intermolecular interactions with neighboring molecules.[46]

For example, the asymmetric and symmetric stretchings of COO^- (in ionic form) for glycine appear at 1610 and 1413 cm^{-1}, respectively, with the separation $\Delta = 197$ cm^{-1}. In the $Ni(gly)_2 \cdot 2H_2O$ complex, with monodentate COO^- coordination to nickel(II) and a hydrogen bond between C═O and the amine group of a neighboring complex, both the asymmetric and symmetric COO^- stretching frequencies decrease (1589, 1411 cm^{-1}), as also does their separation $\Delta = 178$ cm^{-1}. This type of coordination with reduced $\nu_a(COO^-)$ is often classified as "H-bonded monodentate".[45] However, in the octahedrally coordinated $Cd(gly)_2 \cdot H_2O$ complex with monodentate carboxylate coordination to the cadmium(II) ion (Cd−O ∼ 2.3 Å), the $\nu_a(COO^-)$ mode also shifts to a lower frequency (1574 cm^{-1}), as its C═O group forms a bridge to the cadmium(II) ion in a neighboring complex (Cd−O ∼ 2.5 Å).[48] A similar effect is observed in the cadmium(II) penicillamine complex of $[CdBr(HPen)(H_2O)] \cdot 2H_2O$, where the carboxylate group is coordinated in the "asymmetrical bidentate" mode, with Cd−O distances of 2.26 and 2.72 Å, shifting the asymmetric and symmetric COO^- stretching frequencies to 1595 and 1419 cm^{-1} ($\Delta =$ 176 cm^{-1}), relative to the those in the pure ligand (1614 and 1397 cm^{-1}, $\Delta = 217$ cm^{-1}).[8] The antisymmetric and symmetric COO^- stretching vibrations of some amino acid metal complexes are collected in Table S-4 (Supporting Information).[49−52] It has been suggested that $\Delta\nu$ values significantly less than for the ionic form are indicative of chelating or bridging carboxylate groups.[43,44]

The IR-active asymmetric and symmetric COO^- stretching modes of cysteine (ionic form) appear at 1587 and 1394 cm^{-1}, respectively,[29] with $\Delta = 1587 - 1394 = 193$ cm^{-1}. In the IR spectra of **1** and **2**, the $\nu_a(COO^-)$ stretching shifts to a lower wavenumber (1574 cm^{-1}), while the $\nu_s(COO^-)$ shifts slightly to a higher wavenumber (1398 cm^{-1}), with $\Delta = 1574 - 1398 = 176$ cm^{-1}. This small band separation is similar to that in $[CdBr(HPen)(H_2O)] \cdot 2H_2O$, indicating that the carboxylate group is coordinated to the cadmium(II) ion in monodentate mode, or in strongly asymmetrical bidentate mode, as in the cadmium(II) penicillamine complex $[CdBr(HPen)(H_2O)] \cdot 2H_2O$, also with $\Delta = 176$ cm^{-1}.[8] This is also supported by the 0.7 ppm chemical shift of the COO^- group in the ^{13}C NMR spectra of **1** and **2** relative to that in the pure cysteine.

Considering all of the factors, including, (a) the reported ^{113}Cd chemical shifts of 574−645 ppm for CdS_3O geometry, together with 669−707 ppm for CdS_4 sites in the dinuclear metal binding site of the GAL4 transcription factor,[53] and 600−680 ppm for singly bridged CdS_4 sites in cadmium(II)-loaded metallothionein (Cd_7-MT),[34] (b) the fit of the CdS_3O model to the EXAFS oscillations of **1** and **2** and the closeness of the average Cd−S distance 2.52 ± 0.02 Å to those in crystalline cadmium(II) complexes with tetrahedral geometries (CdS_4 and CdS_3O), (c) the splitting of ν_a and ν_s stretching vibrations of the COO^- group ($\Delta\nu = 176$ cm^{-1}) and ^{13}C chemical shift of 0.7 ppm for its carbon atom, (d) the closer similarity of the second derivative of the Cd L_3-edge XANES spectra of **1** and **2** to that of the standard CdS_3O compound than to that of CdS_4, and (e) the low-frequency Raman and far-IR spectra showing bridging and terminal Cd−S vibrational bands, we arrive at a "cyclic/cage" type of structural model, such as **A**, **B**, and **C** in Scheme 2, that can be considered for the cadmium(II) complex in the $Cd(HCys)_2 \cdot H_2O$ compound. The framework of these structures consists of mixed CdS_3O and CdS_4 coordination sites held together by bridging thiolate groups, forming a "cyclic/cage" structure. The thiolate ligands must

(47) Nakamoto, K.; Morimoto, Y.; Martell, A. E. *J. Am. Chem. Soc.* **1961**, *83*, 4528–4532.
(48) Niven, M. L.; Thornton, D. A. *Inorg. Chim. Acta* **1979**, *32*, 205–208.
(49) Condrate, R. A.; Nakamoto, K. *J. Chem. Phys.* **1965**, *42*, 2590.
(50) Gale, R. J.; Winkler, C. A. *Inorg. Chim. Acta* **1976**, *21*, 151–156.
(51) Chandrasekharan, M.; Udupa, M. R.; Aravamudan, G. *Inorg. Chim. Acta* **1973**, *7*, 88–90.
(52) Watt, G. W.; Knifton, J. F. *Inorg. Chem.* **1967**, *6*, 1010–1014.
(53) Gardner, K. H.; Pan, T.; Narula, S.; Rivera, E.; Coleman, J. E. *Biochemistry* **1991**, *30*, 11292–11302.

be shared between the cadmium(II) ions to accommodate the cadmium(II)/thiolate ratio of 1:2. Structures **A** and **B** are similar to those of the Cd_3S_9 and Cd_4S_{11} clusters in Cd_7-MT.[54] For Cd_7-MT, the mean Cd−S distance of 2.53(2) Å has been reported from EXAFS studies,[55,56] as have ^{113}Cd NMR chemical shifts in the range of 600−680 ppm.[34] The "chain" type of structure similar to the one shown in Figure S-11 (Supporting Information) is less likely, because for such a distinct Cd···Cd distance in a doubly bridged oligomer a peak around 3−4 Å would be expected in the Fourier-transformed EXAFS spectrum, as in Figure S-6a (right; Supporting Information).

Conclusion

Two amorphous compounds with cadmium(II)−cysteinate complexes, prepared by reacting cysteine with $Cd(CH_3COO)_2$ and $Cd(ClO_4)_2$ salts, were identified as $Cd(HCys)_2 \cdot H_2O$ (**1**) and $\{Cd(HCys)_2 \cdot H_2O\}_2 \cdot H_3O^+ClO_4^-$ (**2**) using C, H, and N elemental analysis; thermogravimetry−differential scanning calorimetry; and IR and Raman spectroscopy. Vibrational spectra suggest coordination of the cysteinate ligands through the thiolate sulfur atom and also monodentate or strongly asymmetrical bidentate coordination of the carboxylate group, while the protonated ($-NH_3^+$) amine group is not bound. The perchlorate ion in compound **2**, which precipitated at high acidity (pH 1.6), requires H_3O^+ as a counterion. The very weak Raman band at 1736 cm^{-1} indicates hydrogen bonding between the carboxylate and H_3O^+ ions in **2**. The ^{13}C NMR, Cd K-edge EXAFS, and L_3-edge XANES spectra of **1** and **2** are virtually identical, indicating a closely related local structure around the cadmium(II) ion in both complexes. EXAFS data analyses for **1** and **2** by means of least-squares curve-fitting of theoretical model oscillations show an average Cd−S distance of 2.52 ± 0.02 Å. For all refined CdS_xO_y models, CdS_3O resulted in the most reliable parameters, with mean Cd−S and Cd−O distances of 2.52 ± 0.02 and 2.27 ± 0.04 Å, respectively, which are consistent with the average crystallographic bond distances for a distorted tetrahedral CdS_3O coordination. The broad resonances in the solid-state ^{113}Cd NMR with chemical shifts in the 500−700 ppm range and peak maxima around 650 ppm for **1** and **2** are compatible with both CdS_4 and CdS_3O as major coordination sites. The second derivatives of the Cd L_3-edge XANES spectra of **1** and **2** are more similar to that of the standard CdS_3O compound than CdS_4, indicating that the latter cannot be the dominating type of coordination. Therefore, for the hydrated cadmium(II) cysteinate complex in the solid state, a "cyclic/cage" type of structure similar to those in Scheme 2 is proposed, with a framework of CdS_3O and CdS_4 coordination sites (not dominated by CdS_4) held together by bridging thiolate groups, and with coordinated carboxylate oxygen atoms.

In summary, since both ^{113}Cd NMR and EXAFS spectroscopy techniques provide average signals for all of the cadmium(II) coordination sites in the sample, the majority of the cadmium(II) ions in the amorphous cadmium(II)−cysteinate solids **1** and **2** should be in CdS_3O and CdS_4 sites. Scheme 2**A**, **B**, and **C** provide examples of probable structures for the hydrated $Cd(HCys)_2$ complexes. However, other arrangements with single thiolate bridges between the cadmium(II) ions with CdS_3O (dominating) and CdS_4 coordination, together with minor amounts of, for example, CdS_3O_{2-3} and CdS_4O sites cannot be excluded. Even though unusual, combinations of several coordination geometries are found for some solid compounds, for example, CdS_4, CdS_4O, and CdS_3O_3 in the crystal structure of the decanuclear $[Cd_{10}(SCH_2CH_2OH)_{16}](ClO_4)_4 \cdot 8H_2O$ complex.[40]

Acknowledgment. We are grateful to Professor Roderick E. Wasylishen (University of Alberta) for the use of the NMR facility at U of A, to reconfirm the signals in the solid-state ^{113}Cd NMR spectra of **1** and **2**. Beam time was allocated for X-ray absorption measurements at the Photon Factory, Tsukuba, Japan (proposal No. 2005G226) and SSRL, United States of America (proposal No. 2848), which is operated by the Department of Energy, Office of Basic Energy Sciences, U. S. A. The SSRL Biotechnology Program is supported by the National Institutes of Health, National Center for Research Resources, Biomedical Technology Program, and by the Department of Energy, Office of Biological and Environmental Research. We gratefully acknowledge the Natural Sciences and Engineering Research Council (NSERC) of Canada, Canadian Foundation for Innovation (CFI), Alberta Science and Research Investments Program (ASRIP), Alberta Synchrotron Institute (ASI), and the University of Calgary for providing financial support. F.J. is a recipient of the NSERC University Faculty Award (UFA). J.M. and L.H. gratefully acknowledge the Hungarian National Research Foundation (OTKA K61611) for financial

(54) Henkel, G.; Krebs, B. *Chem. Rev.* **2004**, *104*, 801–824.
(55) Jiang, D. T.; Heald, S. M.; Sham, T. K.; Stillman, M. J. *J. Am. Chem. Soc.* **1994**, *116*, 11004–11013.
(56) Abrahams, I. L.; Garner, C. D.; Bremner, I.; Diakun, G. P.; Hasnain, S. S. *J. Am. Chem. Soc.* **1985**, *107*, 4596–4597.
(57) Henehan, C. J.; Pountney, D. L.; Zerbe, O.; Vašák, M. *Protein Sci.* **1993**, *2*, 1756–1764.
(58) Lee, H. J.; Lian, L.-Y.; Scrutton, N. S. *Biochem. J.* **1997**, *328*, 131–136.
(59) Luczkowski, M.; Stachura, M.; Schirf, V.; Demeler, B.; Hemmingsen, L.; Pecoraro, V. L. *Inorg. Chem.* **2008**, *47*, 10875–10888.
(60) Pan, T.; Freedman, L. P.; Coleman, J. E. *Biochemistry* **1990**, *29*, 9218–9225.
(61) Coleman, J. E. In *Methods in Enzymology vol. 227: Metallobiochemistry, Part D*; Riordan, J. F., Valee, B. L., Eds.; Academic Press: San Diego, CA, 1993; pp 16−43.
(62) Lee, K.-H.; Cabello, C.; Hemmingsen, L.; Marsh, E. N. G.; Pecoraro, V. L. *Angew. Chem., Int. Ed.* **2006**, *45*, 2864–2868.
(63) Iranzo, O.; Cabello, C.; Pecoraro, V. L. *Angew. Chem., Int. Ed.* **2007**, *46*, 6688–6691.
(64) Peacock, A. F. A.; Hemmingsen, L.; Pecoraro, V. L. *Proc. Natl. Acad. Sci. U. S. A.* **2008**, *105*, 16566–16571.
(65) Li, X.; Suzuki, K.; Kanaori, K.; Tajima, K.; Kashiwada, A.; Hiroaki, H.; Kohda, D.; Tanaka, T. *Protein Sci.* **2000**, *9*, 1327–1333.
(66) Gruff, E. S.; Koch, S. A. *J. Am. Chem. Soc.* **1990**, *112*, 1245–1247.
(67) Santos, R. A.; Gruff, E. S.; Koch, S. A.; Harbison, G. S. *J. Am. Chem. Soc.* **1991**, *113*, 469–475.
(68) Xiao, Z.; Lavery, M. J.; Ayhan, M.; Scrofani, S. D. B.; Wilce, M. C. J.; Guss, J. M.; Tregloan, P. A.; George, G. N.; Wedd, A. G. *J. Am. Chem. Soc.* **1998**, *120*, 4135–4150.
(69) Dołega, A.; Baranowska, K.; Gajda, J.; Kaźmierski, S.; Potrzebowski, M. J. *Inorg. Chim. Acta* **2007**, *360*, 2973–2982.
(70) Maitani, T.; Suzuki, K. T. *Inorg. Nuclear Chem. Lett.* **1979**, *15*, 213–217.
(71) Darensbourg, D. J.; Niezgoda, S. A.; Draper, J. D.; Reibenspies, J. H. *J. Am. Chem. Soc.* **1998**, *120*, 4690–4698.

support and thank Dr. J. Mihály, Cs. Németh and L. Kocsis (Chemical Research Center of HAS, Budapest, Hungary) for their assistance in spectroscopic experiments.

Supporting Information Available: Raman spectra of **1**, **2**, and solid cysteine (200−3000 cm^{-1}); assignment of the vibrational bands for cysteine, **1**, and **2** (1100−3000 cm^{-1}); comparison between EXAFS spectra of **1** and **2**; EXAFS curve-fitting results for **2** using different models; EXAFS spectra of bis(cysteaminate) cadmium(II) and $(Et_3NH)_4[S_4Cd_{10}(SPh)_{16}]$ cadmium adamantane cage and corresponding Fourier transforms; structure of crystalline $CdS_x(N/O)_y$ model compounds used as standards for Cd L_3-edge XANES measurements; ^{113}Cd NMR spectra of $[Cd(thiourea)_2(NO_3)_2]$ and $[Cd(thiourea)_2(HCOO)_2]$; results from the crystal structure database survey of $CdS_x(N/O)_y$ complexes and their structures. This material is available free of charge via the Internet at http://pubs.acs.org.

IC900145N